Structural Monitoring and Maintenance, *Vol. 7, No. 1 (2020) 1-12*
DOI: https://doi.org/10.12989/smm.2020.7.1.001

Continuous deformation measurement for track based on distributed optical fiber sensor

Jianping He*[1], Peigang Li[1,2] and Shihai Zhang[3]

[1]*School of Civil Engineering, Dalian University of Technology, Dalian 116024, P.R. China*
[2]*Faculty of Railway Transportation, Shanghai Institute of Technology, Shanghai 201418, P.R. China*
[3]*School of Civil Engineering, Nanyang Institute of Technology, Nanyang 473001, P.R. China*

(Received June 7, 2019, Revised August 6, 2019, Accepted August 15, 2019)

Abstract. Railway tracks are the direct supporting structures of the trains, which are vulnerable to produce large deformation under the temperature stress or subgrade settlement. The health status of track is critical, and the track should be routinely monitored to improve safety, lower the risk of excess deformation and provide reliable maintenance strategy. In this paper, the distributed optical fiber sensor was proposed to monitor the continuous deformation of the track. In order to validate the feasibility of the monitoring method, two deformation monitoring tests on one steel rail model in laboratory and on one real railway tack in outdoor were conducted respectively. In the model test, the working conditions of simply supported beam and continuous beam in the rail model under several concentrated loads were set to simulate different stress conditions of the real rail, respectively. In order to evaluate the monitoring accuracy, one distributed optical fiber sensor and one fiber Bragg grating (FBG) sensor were installed on the lower surface of the rail model, the strain measured by FBG sensor and the strain calculated from FEA were taken as measurement references. The model test results show that the strain measured by distributed optical fiber sensor has a good agreement with those measured by FBG sensor and FEA. In the outdoor test, the real track suffered from displacement and temperature loads. The distributed optical fiber sensor installed on the rail can monitor the corresponding strain and temperature with a good accuracy.

Keywords: distributed optical fiber sensor; structural health monitoring; deformation measurement; temperature compensation; track

1. Introduction

As the rapid development of urbanization and the promotion of "the Belt and Road (B&R)", the railway construction, especially the high-speed railway construction in China, has grown rapidly in the world. With the great rising of the speed, it is very important for the ride comfort and safety of the train. Railway tracks are the direct supporting structures of the train, and they are being exposed to various adverse conditions such as subgrade settlement, high and low temperature cyclic load. Over time, these factors can lead to large deformation of rail and then influence the driving safety. Track deformation is usually regarded as an important index for the safety assessment. In fact, many decisions regarding remedial intervention are generally taken when the deformation has exceeded a previously established threshold. For example, when rail deformation is small, rail fasteners can be

*Corresponding author, Ph.D., E-mail: hejianp@dlut.edu.cn

http://www.techno-press.org/?journal=smm&subpage=7 ISSN: 2288-6605 (Print), 2288-6613 (Online)

adjusted. Therefore, researching an efficient, real-time monitoring method to detect the state of track is of great significance to ensure the safe operation, lower the risk of excess deformation and provide reliable maintenance strategy of the high speed railways.

At present, inspection and monitoring methods are the two main methods to evaluate the damage of the track. Track inspection methods include flaw detection and irregularity detection, which have given priority to use detection car instrumented with flaw detector or some other sensing equipments. These methods can directly find the damage in the track, but they cannot achieve real-time monitoring, which only detect the track state at the comprehensive maintenance window's length of high-speed railway (Xu 2017, Li 2011). To improve the real-time and reliability of safety evaluation, some researchers have focused on the settlement monitoring of subgrade. Rail deformation often is caused by the subgrade settlement, so track deformation can be indirectly evaluated by the state of subgrade. The settelment monitoring methods include GPR (ground-penetrating radar), InSAR (Synthetic Aperture Radar Interferometry), TDR (Time domain reflectometry) and BOTDR (Brillouin optical time domain reflectometry) (Francisco 2011, Yang 2010, Jiang 2011). Jiang et al. used BOTDR system to monitor the karst soil cave (Jiang 2006); Xu and He also used distributed strain data measured by BOTDR system to predict collapse prediction of karst sinkhole by using distributed Brillouin optical fiber sensor packaged by FRP (fiber reinforced polymer) (Xu and He 2016). These monitoring methods can effectively monitor the settlement, but they cannot directly describe the track deformation. Some direct monitoring techniques such as magnetic flux leakage (MFL) method (Antipov 2018) and fiber Bragg grating (FBG) sensing techniques have been proposed to monitor the rail damage. Wang et al. used FBG strain sensor to measure the temperature force of long seamless rails (Wang 2016). Li et al. developed one rail expansion devices based on FBG sensors on an urban railway viaduct, the monitoring items include rail temperature, rail displacement and strain of sliding rail (Li 2014). These methods cannot cover the global range due to their limited location monitoring. The distributed Brillouin optical fiber sensing technology is one of the most promising measuring technologies for the direct deformation measurement of track, and there is not much of this kind of research on track deformation monitoring at present.

In this paper, the distributed optical fiber sensor was applied to monitor the continuous deformation of the track. Firstly, one deformation measurement test for a steel track model with the length of 6m was conducted in Lab, on the lower surface of which one distributed optical fiber sensor and one FBG sensor were installed. In this test, one simple support working condition and one continuous working condition were setup to validate the effectiveness of the deformation monitoring method, and several concentrated loads and symmetrical load were loaded on the track model to produce deformation respectively. A comparison study among the measured strain from the distributed optical fiber sensor, that from the local FBG sensor and that calculated by FEA was conducted. Then, one distributed optical fiber sensor with the length of 48m was installed on the surface of one real track for deformation measurement, on which artificial displacement loads and ambient temperature were loaded.

2. Principle of the distributed Brillouin optical fiber sensing technology

Based on the analysis of the Brillouin scattering spectrum, we can know that the Brillouin frequency shift is linear with both the strain and the temperature, which can be described by

$$\Delta\nu_B = C_\varepsilon \Delta\varepsilon + C_T \Delta T \tag{1}$$

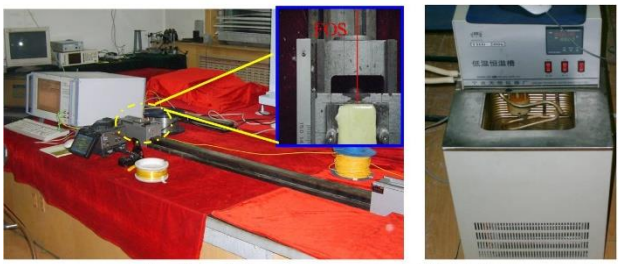

Fig. 1 Strain and temperature sensing calibration tests

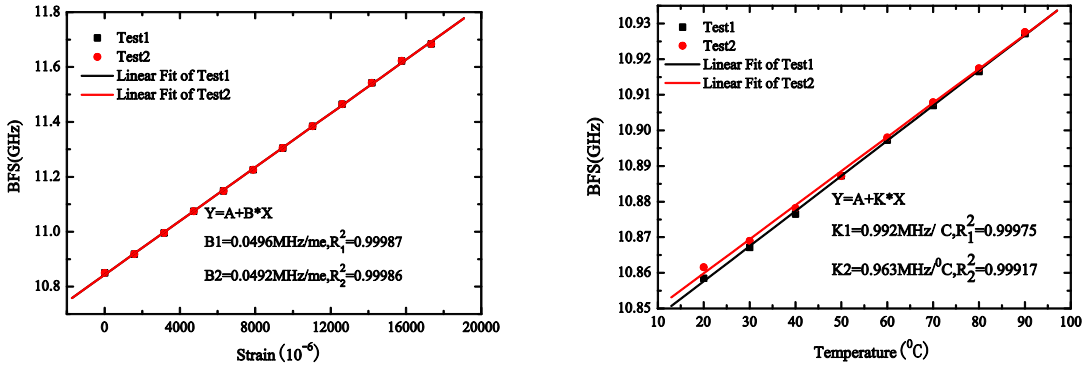

(a) Result of strain sensitivity coefficient (b) Result of temperature sensitivity coefficient

Fig. 2 The results of sensing calibration test for corning optical fiber

where C_ε, C_T denote the strain and temperature sensitivity coefficients respectively, and $\Delta\varepsilon, \Delta T$ denote the strain and temperature increment (Culverhouse 1989, Horiguchi 1990). In the lab, the strain and temperature sensing tests for corning optical fiber were conducted as illustrated in Fig.1. The strain and temperature sensitivity coefficients are 0.05MHz/με and 1.00MHz/℃ respectively, as shown in Fig. 2.

As illustrated in Eq. (1), the Brillouin frequency shift is a function of strain and temperature, and it is necessary to remove the cross-sensitivity of the distributed Brillouin strain fiber optical sensor in field applications. In order to eliminate the measuring errors induced by the change of temperature, one distributed Brillouin temperature fiber optical sensor should be installed parallel to the distributed Brillouin strain fiber optical sensor. The temperature compensation method can be expressed

$$\Delta\varepsilon = (\Delta\nu_B - \psi\Delta\nu_{B1})/C_\varepsilon \tag{2}$$

where $\Delta\nu_{B1}$ ($\Delta\nu_{B1} = C_{TT}\Delta T$) and C_{TT} are the Brillouin frequency shift and the temperature sensing coefficient of Brillouin temperature fiber optical sensor, $\psi = C_T / C_{TT}$.

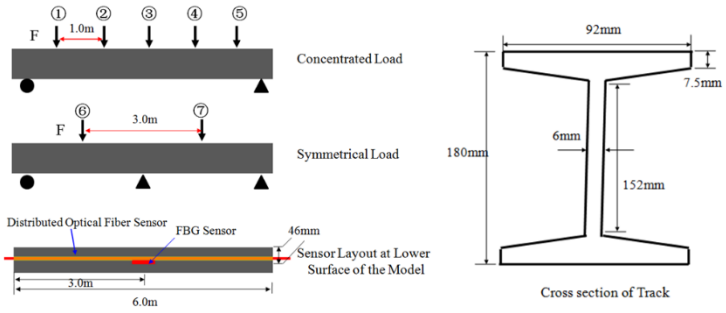

Fig. 3 Track model and sensor layout

3. Deformation measurement test for a steel track model

3.1 Experimental setup

Fig. 3 shows the diagram of the steel track model with the length of 6m. In the figure, one simple support working condition and one continuous support working condition were setup respectively. In the simple support working condition, the span was 5.7 m and several concentrated loads were loaded. The moment of inertias (i_x, i_y) and the section modulus (w_x, w_y) are 1660 cm^4, 122 cm^4, 185 cm^3 and 26 cm^3 respectively. In the continuous support working condition, each span was 2.85 m and several symmetrical loads were loaded on the middle point of each span. In order to simulate the deformation of the track model at different positions, several levels of concentrated loads and symmetrical loads were set as illustrated in this figure. In the figure, the numbers ①-⑦ denote the load positions. Among these load positions, the numbers from ① to ⑤ denote the concentrated loads applied on the simple support track, respectively; the numbers of ⑥ and ⑦ denote the symmetrical loads applied on the continuous rail model respectively. All the other loads include several stage loads:0 kN, 6.67 kN, 13.33 kN, 20 kN, 26.67 kN and 33.34 kN.

Fig. 4 The photo of experimental setup

In order to measure the deformation of the track model, one bare single mode optical fiber was continuously glued on the bottom surface of the track. By comparison, one local FBG sensor with the initial wavelength of 1535.768 nm was glued at the middle point of the bottom surface of the track. To prepare the track model for sensor installation, sandpapers with different models were used to remove irregularities on the surface of rail model and provide a smooth and uniform surface.

The distributed strain was measured by the Brillouin sensing system with the spatial resolution of 500 mm and the sampling distance of 100 mm; the local strain at the middle point of the track was measured by the FBG system with the accuracy of 2pm. Fig. 4 shows the photo of experimental setup in the laboratory. In the laboratory, there was little change in ambient temperature, so temperature compensation for strain measurement was not considered.

3.2 Experimental results

Fig. 5 shows the finite element conclusion of the rail track model at the simple support working condition under the load of 20kN. The load position is according to the load ③. The finite element model of the rail track model was setup by the ABQUS with the spatial two-node linear beam element. The element type, the element size and the numbers of element and material model are B31, 0.15 m and 42 in the FEA model. The density, elasticity modulus, poisson's ratio and yield stress of the steel track model are 7850kg/m^3, 210GPa, 0.3 and 0.345GPa respectively.

Figs. 6 and 7 show the resulting tensile strain distributions along the Brillouin fiber optical sensor corresponding to the applied load steps. Before that the load was applied on the rail model, a zero-strain reading was recorded as the reference strain by the Brillouin sensing system and FBG system respectively. The load was gradually increased, the Brillouin frequency shift and center wavelength were recorded at each stage of load. The concentrated load positions are 2m and 1m from the middle point of rail model. It can be seen that the measured strain curves have good symmetries at the symmetric load position.

Fig. 8 shows the measured strain distributions, the theoretical (or reference) strain distributions and the strain distribution calculated from FEA corresponding to the load steps, and the load position was Load-③. It can be seen that the theoretical strain was slightly larger than that measured by the distributed Brillouin fiber optical sensor at each stage.

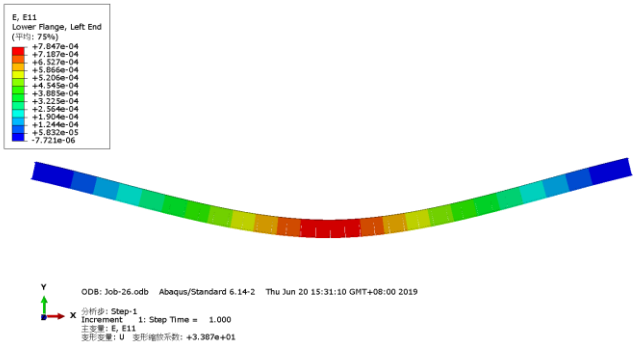

Fig. 5 The finite element conclusion of the rail track model at simple support working condition

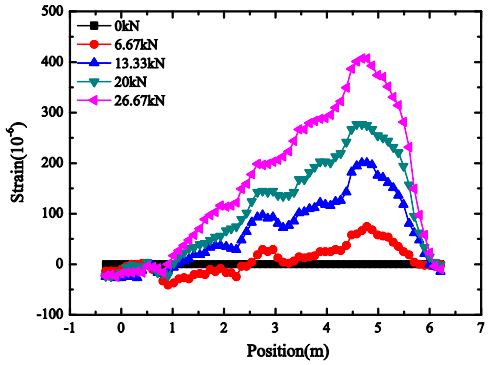

(a) At Load-⑤

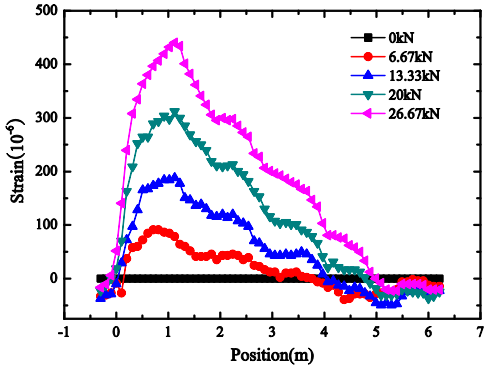

(b) At Load-①

Fig. 6 Strain measurement data under concentrated Load-① and Load-⑤

The reason is that the accuracy of the strain measurement from Brillouin system is strongly affected by the spatial resolution, that is, the short distance over which the sensor is capable of measuring an average strain. In this work, the BOTDA (Brillouin optical time domain analysis) system with the measuring accuracy of ±50με and the spatial resolution of 50cm was used to measure the strain data. Fig. 9 shows the strain comparison at the position of midspan measured from FBG sensor, distributed Brillouin fiber optical sensor, theoretical calculation and FEA under the concentrated loads of 20kN. It can be seen that the comparison between the strain collected by FBG, the reference strain and FEA conclusion also shows a good agreement and those collected by the distributed Brillouin fiber optical sensor are slightly smaller than the reference strains at different level of loads. The maximum relative errors between reference strain and those measured by FBG and distributed Brillouin optical fiber sensor are 1.79% and 5.02% respectively.

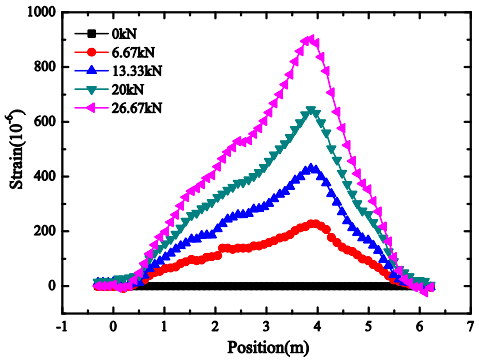

(a) At load-④

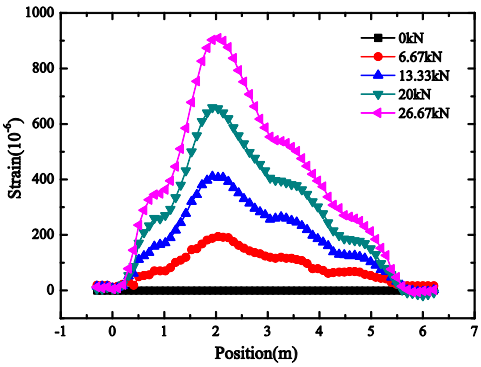

(b) At load-②

Fig. 7 Strain measurement data under concentrated Load-② and Load-④

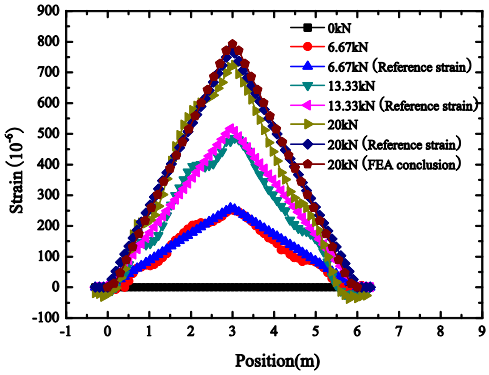

Fig. 8 Stain distributed under load-③

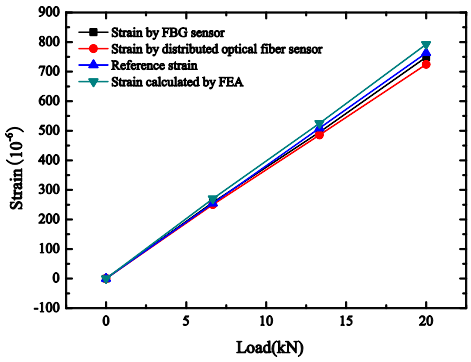

Fig. 9 Strain comparison of FBG sensor, distributed optical fiber sensor, theoretical and FEA conclusion

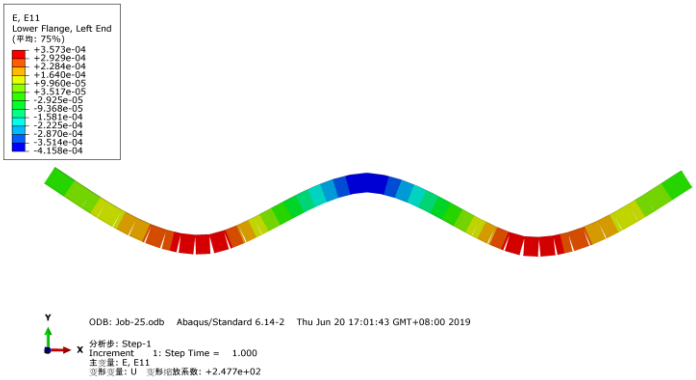

Fig. 10 The finite element conclusion of the rail track model at continuous support working condition

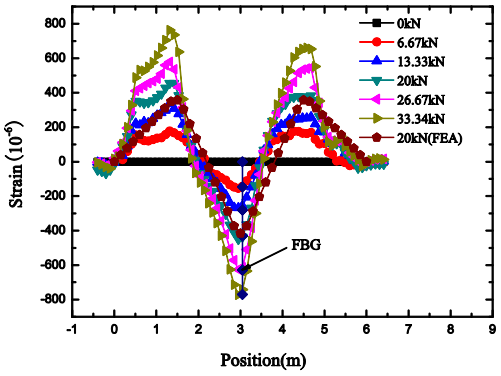

Fig.11 Strain measurement data under symmetrical loads

Fig. 10 shows the result of FEA conclusion of the track model at continuous support working condition under the concentrated load of 20 kN, and the load positions were Load-⑥ and Load-⑦. Fig. 11 shows the measured results of the distributed Brillouin fiber optical sensor and FEA conclusion under different level of symmetrical loads. For the continuous rail model, the bending moment at the position of intermediate support is negative under the vertical load, and the measured strain curves show good symmetrical. It can be seen that the comparison between the strain collected by FBG, the distributed n fiber optical sensor and the FEA conclusion also shows a good agreement, the maximum strain difference between from the two sensors and from FEA conclusion is less than 40με.

4. Deformation monitoring test for a real railway track

Fig. 12 shows the deformation monitoring test for a real railway track located in Shanghai, China and carried out in December 2018. One optical fiber sensor with length of 48 m was installed on the track for strain measurement as shown in Fig. 12(b). The distance between the two rail fastening devices is 65 cm. In order to produce deformation, three adjacent rail fastening devices were removed as shown in Fig. 12(c), and the track was loaded upward displacement as shown in Fig. 12 (d). Fig. 13 shows the test diagram. The sensor installed on the track was connected to the Brillouin sensing system by using one transmission optical cable with the length of 20 m.

The upward displacements of the track were 0mm (initial displacement), 5 mm, 10 mm and 15 mm measured by micrometer and the strain produced on the track was measured by the distributed optical fiber sensor at each level load. Fig. 14 shows the distribution of the Brillouin frequency shift at each level displacement. It can be seen that the position of the load point is about 35 m. In the figure, the "0" point represents the starting point of the optical fiber sensor installed on the track. The whole measuring process, the ambient temperature was maintained at about 5.3°C, so temperature compensation was not conducted.

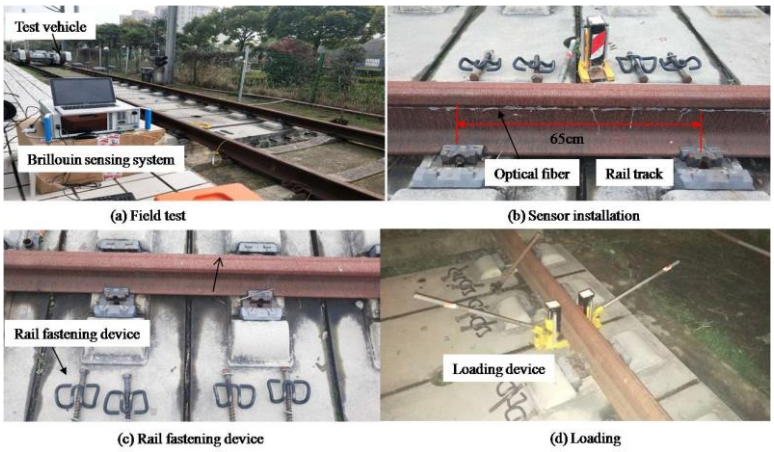

Fig. 12 The deformation monitoring test for a real railway track

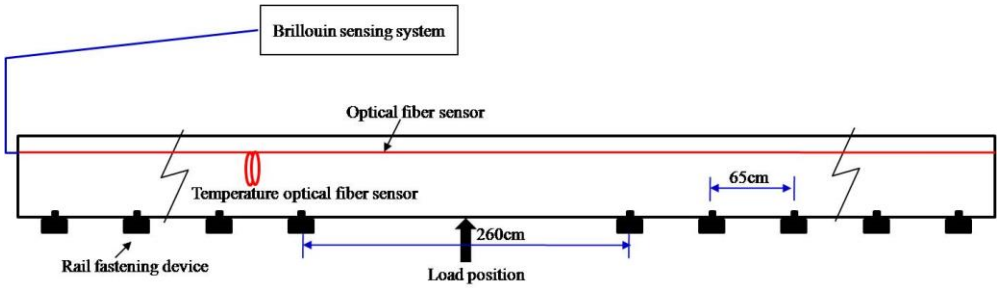

Fig. 13 Test diagram

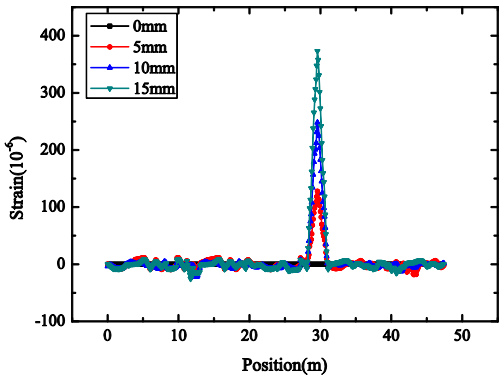

Fig. 14 Strain distribution of rail track under different level displacements

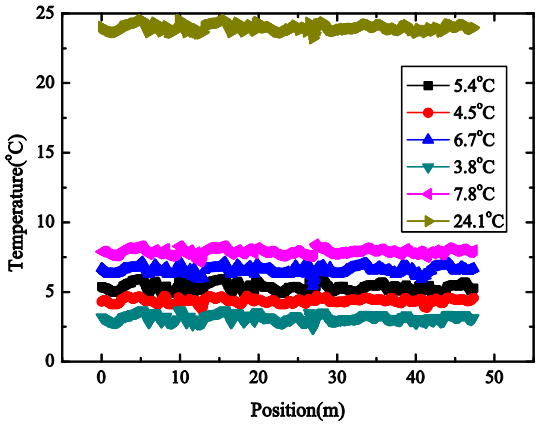

Fig. 15 Temperature distribution of rail track under different ambient temperature

Fig.15 shows the temperature state of the track at six different times, and the corresponding ambient temperatures were 5.4ºC, 4.5ºC, 6.7ºC, 3.8ºC, 7.8ºC and 24.1ºC respectively. In the whole measuring process, the track only bored the ambient temperature load, that is, the optical fiber installed on the track only sensed the temperature. It can be seen that the temperature of track measured by the optical fiber sensor agrees well with the ambient temperature.

5. Conclusions

This paper has presented the use of the distributed Brillouin fiber optical sensor to measure the deformation of the track, and the feasibility of the monitoring method was validated by one indoor model test and outdoor real track test respectively. In the model test, both the strain measured one FBG sensor installed on the lower surface of the track model and that calculated by FEA are also applied as the measurement references of the distributed optical fiber sensor. Results reveal that the distributed optical fiber sensor can monitor the strain distribution of the track model and the strain distribution show a good agreement with both that calculated by FEA and that measured by the FBG sensor at the position of the FBG sensor. In the outdoor test, the real track suffered from different level of displacement loads and ambient temperature load. Strain monitoring results show that the distributed optical fiber sensor can measure the strain distribution of the real track. It also can be seen that the distributed optical sensor can be very sensitive to the ambient temperature which indicates that temperature compensation for strain measurement must be done in field applications. The initial study has proved the feasibility of distributed fiber optical sensor to measure the deformation of track. In this work, the sensor was installed on the track by using glue, and the bond strength between the sensor and the track may fail under the action of vibration caused by the high-speed track. In the future study, some novel sensor layout methods will be studied to ensure the reliability of monitoring, the quick sensor installation and the maintainability of sensors for the in-service rail.

Acknowledgments

The research described in this paper was financially supported by the National Key Research and Development Program of China (2016YFC0701107), the National Natural Science Foundation of China (No. 61875027and No.61675102). The authors are grateful for Dalian Boruixin Co.,LtD. who has provided the Brillouin and FBG sensing equipments for the tests.

References

Antipov, A.G. and Markov, A.A. (2018), "3D simulation and experiment on high speed rail MFL inspection", *Ndt&E Int*, **96**, 177-185. https://doi.org/10.1016/j.ndteint.2018.04.011.

Culverhouse, D. and Farahi, F. (1989), "Potential of stimulated Brillouin scattering as sensing mechanism for distributed temperature sensors", *Electron. Lett.*, **25**, 913-915. https://doi.org/10.1049/el:19890612.

Francisco, G., Jorge, P.G. and Pedro, L. (2011), "Integrating geomorphological mapping, trenching, InSAR and GPR for the identification and characterization of sinkholes: a review and application in the mantled evaporate karst of the Ebro Valley", *Geomorphology*, **132**, 144-156. https://doi.org/10.1016/j.geomorph.2011.01.018.

Horiguchi, T. Kurashima, T. and Tateda, M. (1990), "A technique to measure distributed strain in optical fibers", *IEEE Photonic Tech. L.*, **23**, 52-354. https://doi.org/10.1109/68.54703.

Jiang X.Z., Lei, M.T. and Chen, Y. (2006), "An experiment study of monitoring sinkhole collapse by using BOTDR fiber optical sensing technique", *Hydrogeol. & Eng. Geol. (Chinese)*, **33**(6), 172-176. https://doi.org/10.3969/j.issn.1000-3665.2006.06.019.

Jiang X.Z., Lei, M.T. and Dai, J.L. (2011), "A study of the monitoring deformation of sinkhole collapse using TDR time domain reflectometry", *Hydrogeol. & Eng. Geol. (Chinese)*, **38**(1), 118-121. https://doi.org/10.3969/j.issn.1000-3665.2011.01.022.

Li, W.L., Pang, J. and Lu, X.S. (2014), "Rail expansion devices monitored by FBG sensors on an urban railway viaduct", *Photonic Sens.*, **4**(2),173-179. https://doi.org/10.1007/s13320-014-0163-6.

Li, Z., Dollevoet, R., Molodova, M. and Zhao, X. (2011), "Squat growth–some observations and the validation of numerical predictions", *Wear*, **271**, 148-157. https://doi.org/10.1016/j.wear.2010.10.051.

Wang, P., Xie, K. and Chen, R. (2016), "Test verification and application of a longitudinal temperature force testing method for long seamless rails using FBG strain sensor", *J. Sensors*, **4**, 1-11. https://doi.org/10.1155/2016/3917604.

Xu, J. and He, J.P. (2016), "Collapse prediction of karst sinkhole via distributed Brillouin fiber optical sensor", *Meas.*, **100** ,68-71. https://doi.org/10.1016/j.measurement.2016.12.046

Xu, L. and Zhai, W.M. (2017), "A novel model for determining the amplitude-wavelength limits of track irregularities accompanied by a reliability assessment in railway vehicle-track dynamics", *Mech. Syst. Signal Pr.*, **86**, 260-277. https://doi.org/10.1016/j.ymssp.2016.10.010.

Yang, C.S., Zhang, Q. and Zhao, C.Y. (2010), "Monitoring mine collapse by D-InSAR", *M.S.Tech (Chinese)*, **20**, 696-700. https://doi.org/10.1016/S1674-5264(09)60265-9.

TY